

1
2
3
4
5
6
7
8
9
10
11
12
13
14
15
16
17
18
19
20
21
22
23
24
25
26
27
28
29
30
31
32
33
34
35
36
37
38
39
40
41
42
43
44
45
46
47
48
49
50

Decoupling between the Temperature-Dependent Structural Relaxation and Shear Viscosity of Concentrated Lithium Electrolyte

Tsuyoshi Yamaguchi,^{a,†} Koji Yoshida,^b Toshio Yamaguchi,^b Michihiro Nagao,^{c,d} Antonio Faraone,^c
and Shiro Seki^{e,‡}*

^a Department of Molecular Design and Engineering, Graduate School of Engineering, Nagoya
University, Furo-cho, Chikusa, Nagoya, Aichi 464-8603, Japan

^b Department of Chemistry, Faculty of Science, Fukuoka University, Nanakuma, Jonan, Fukuoka 814-
0180, Japan

^c NIST Center for Neutron Research, National Institute of Standards and Technology, Gaithersburg,
Maryland 20899-6102, USA

^d Center for Exploration of Energy and Matter, Indiana University, Bloomington, Indiana 47408-1398,
USA

[†] Present Address: Department of Materials Process Engineering, Graduate School of Engineering,
Nagoya University

[‡] Present Address: Department of Environmental Chemistry and Chemical Engineering, School of
Advanced Engineering, Kogakuin University

1^e Materials Science Research Laboratory, Central Research Institute of Electric Power Industry (CRIEPI),

2
3 2-11-1, Iwado-kita, Komae, Tokyo 201-8511, Japan

4
5
6 E-mail: yamaguchi.tsuyoshi@material.nagoya-u.ac.jp (T. Yamaguchi)

7
8
9 CORRESPONDING AUTHOR: E-mail: yamaguchi.tsuyoshi@material.nagoya-u.ac.jp, Tel: +81-52-
10
11 789-3592, Fax: +81-52-789-3273.
12
13
14
15
16
17
18
19
20
21
22
23
24
25
26
27
28
29
30
31
32
33
34
35
36
37
38
39
40
41
42
43
44
45
46
47
48
49
50
51
52
53
54
55
56
57
58
59
60

Abstract

1
2
3
4
5
6
7 The intermediate scattering functions of concentrated solutions of LiPF_6 in propylene carbonate (PC)
8 were measured at various temperatures, two different wavenumbers, and three different concentrations
9 using neutron spin echo (NSE) spectroscopy. The temperature dependence of the relaxation time was
10 larger than that of the steady-state shear viscosity in all the cases. The shear relaxation spectra were also
11 determined at different temperatures. The normalized spectra reduced to a master curve when the
12 frequency was multiplied by the steady-state shear viscosity, indicating that the temperature dependence
13 of the steady-state shear viscosity can be explained by that of the relaxation time of the shear stress. It is
14 thus suggested that the dynamics of the shear stress is decoupled from the structural dynamics at the
15 molecular scale.
16
17
18
19
20
21
22
23
24
25
26
27
28
29
30
31
32
33
34
35
36
37
38
39
40
41
42
43
44
45
46
47
48
49
50
51
52
53
54
55
56
57
58
59
60

1. Introduction

Shear viscosity is a transport property of liquids that governs macroscopic flows. In addition, microscopic dynamic processes in liquids have also been related to the shear viscosity. It is thus of both practical and academic importance to understand the microscopic mechanisms that determine the shear viscosity.

According to the Kubo-Green theory, the steady-state shear viscosity is given by the time-integral of the time correlation function of the shear stress.^{1,2} It is thus approximately proportional to the relaxation time of the fluctuation of the shear stress, and an important question which remains is what are the microscopic modes that are coupled to the shear stress.

One of the important candidates is the density mode at the wavenumber of the main peak of the static structure factor. The structure factor of simple liquids shows a peak at the wavenumber that corresponds to the reciprocal of the intermolecular contact distance, which is called "main peak" in this work.¹ The relaxation of the intermediate scattering function is slow at the main peak, which is well-known as the de Gennes narrowing. The mode-coupling theory (MCT) predicts that the slow dynamics of simple viscous liquids, including the shear relaxation, is governed by the structural relaxation at the main peak.³

The relaxations of the isotropic and the anisotropic parts of the stress tensor, which are related to the bulk and the shear viscosity, respectively, have been studied on various viscous liquids using ultrasonic techniques.⁴ They have been traditionally called "structural relaxation" under the consideration that they originate from the relaxation of microscopic density modes. However, the actual relation between the relaxations of the stress tensor and the density mode is still an open question.

The intermediate scattering function can be measured experimentally using quasi-elastic scattering techniques such as neutron spin-echo (NSE) spectroscopy.^{5,6,7,8,9,10,11,12} The structural relaxation of some viscous liquids was actually determined at the main peak, and the temperature dependence of the relaxation time was usually compared with that of the steady-state shear viscosity. Both quantities were proportional to each other in most cases, while Pravel and coworkers reported the stronger temperature

1 dependence of the structural relaxation time than that of the steady-state shear viscosity in the case of a
2 concentrated solution of LiCl in D₂O.^{11,10}
3
4

5 The relationship between the structural relaxation time and the steady-state shear viscosity has also
6 been a target of computational works on supercooled liquids. Some studies reported that the
7 temperature dependence of the steady-state shear viscosity was stronger than that of the relaxation time
8 of the intermediate scattering function at the main peak, although the self-part of the intermediate
9 scattering function was used in these studies instead of the collective part.^{13,14}
10
11
12
13
14
15

16 We have reported the intermediate scattering functions of a concentrated lithium electrolyte, the
17 solution of LiPF₆ in propylene carbonate (PC), at 298 K and various concentrations, which were
18 determined experimentally using NSE spectroscopy.¹⁵ The results were compared with the frequency-
19 dependent shear viscosity, and it was suggested that the shear relaxation was governed by the structural
20 dynamics at the main peak. In this work, we present the temperature dependence of the structural
21 relaxation time, which is also compared with that of the steady-state shear viscosity. The temperature
22 dependence of the shear relaxation spectra was also measured in order to examine the relationship
23 between the steady-state shear viscosity and the shear relaxation time.
24
25
26
27
28
29
30
31
32
33
34

35 PC is a representative model solvent for a lithium ion battery, and the shear viscosity of the lithium
36 ion electrolyte is a physicochemical quantity that is correlated with the ionic mobility.^{16,17} The
37 temperature dependence of the electrolyte is thus of practical importance for the use of the battery under
38 cold condition. In addition to the results on the solution of the lithium salt, we present the structural
39 dynamics of neat PC, which is a typical example of molecular supercooled liquids. Its dynamics has
40 been studied in various ways¹⁸ such as dielectric spectroscopy,^{19,20} Brillouin scattering²¹ and diffusion
41 measurement.²² We thus consider that the insights obtained by our present work is not limited to
42 electrolyte solutions, but extend to the dynamics of supercooled liquids in general.
43
44
45
46
47
48
49
50
51
52
53
54
55
56
57
58
59
60

2. Experimental[§]

The materials and the methods for the NSE measurement were described in detail in our previous paper.^{15,44} Briefly, LiPF₆ (Kishida Chemical) was dissolved into PC-*d*₆ (CDN Isotope) with the concentrations of 0 (neat PC), 1 mol/kg, 2 mol/kg and 3 mol/kg. These samples were mixed and loaded in Al cylindrical sample cell with a sample thickness of 1 mm in a He atmosphere with a moisture control. The sample temperature was controlled using a top-loading closed cycle refrigerator with a temperature accuracy within ±1 K at the NGA-NSE beam line at the NIST Center for Neutron Research.²³ Using incoming neutron wavelength, λ , of 0.5 nm with a wavelength distribution of about 20%, we measured normalized intermediate scattering function, $I(Q,t)/I(Q,0)$, from the samples at $Q = 10 \text{ nm}^{-1}$ and 14 nm^{-1} in the Fourier time, t , range from 5 ps to 10 ns, where Q denotes momentum transfer, $Q = 4\pi\sin(\theta/2)/\lambda$ with θ the scattering angle. The sample scattering at a base temperature (10 K) was used as a resolution function for the instrument. The DAVE software was used to correct for the instrumental resolution and to obtain $I(Q,t)/I(Q,0)$.²⁴ Error bars represent ±1 standard deviation throughout the paper.

The protonated solvent, PC-*h*₆, was used for the measurements of the steady-state shear viscosity and the shear relaxation spectra. The temperature dependence of the density and the steady-state shear viscosity was measured using two different Stabinger-type viscometers, namely, SVM3000G2 (Anton Paar) at CRIEPI and SVM3001 (Anton Paar) at Nagoya University. The former was used for the solutions of 1 mol/kg, 2 mol/kg, and 3 mol/kg at the temperatures between 283 K and 353 K. The latter was applied to neat PC in addition to the three concentrations noted above. The temperatures of the measurement were below 303 K for solutions and below 313 K for the neat solvent. The agreement of

[§] Certain trade names and company products are identified in order to specify adequately the experimental procedure. In no case does such identification imply our recommendation or endorsement, nor does it imply that the products are necessarily the best for the purpose.

1 the values determined by the two facilities was within 5 % in the overlapping temperature region. The
2 validity of the measured viscosity of neat PC was confirmed by the agreement with the values reported
3 in the literature.^{25,26}
4
5
6

7 We would like to comment here on the H/D substitution effect on the shear viscosity of PC. It is well-
8 known that the H/D substitution modifies both equilibrium and dynamic properties of liquid water,²⁷ and
9 the isotopic effects are ascribed to the strengthening of the hydrogen-bonding upon deuteration. In the
10 case of PC, however, all the hydrogen atoms substituted are C-H protons which do not form hydrogen
11 bond. In the case of liquid benzene, for example, the increase in the shear viscosity upon deuteration is
12 several percent, which is approximately explained by the increase in the total mass.²⁸ We thus consider
13 that the variation of the shear viscosity upon the deuteration of PC is marginal to affect the discussion in
14 this work.
15
16
17
18
19
20
21
22
23
24

25 The shear relaxation spectra of the solutions were measured at 2 mol/kg and 3 mol/kg. The
26 temperatures of the measurements were 298 K, 280 K, 260 K and 250 K for 2 mol/kg solution, while
27 320 K, 310 K, 298 K, 290 K, 280 K and 270 K for 3 mol/kg solution. The experimental methods and
28 devices were described in detail in the literature.^{29,30,31} The frequency range was between 5 MHz and
29 205 MHz. The temperature of the sample was controlled by flowing water through the sample cell at
30 the temperatures above 273 K. The stability of the temperature was within ± 0.2 K. Silicone oil was
31 used as a thermostat fluid instead of water below 273 K, and the temperature stability was within ± 0.5
32 K. The standard errors in the complex shear relaxation spectra, $\eta(\nu)$, were $|\delta\eta(\nu)/\eta_0| < 0.1$ in the
33 frequency region between 15 MHz and 95 MHz, and $|\delta\eta(\nu)/\eta_0| < 0.2$ at other frequencies, where η_0
34 stands for the steady-state shear viscosity.
35
36
37
38
39
40
41
42
43
44
45
46
47
48
49
50
51
52
53
54

55 3. Results and Discussion

56
57
58
59
60

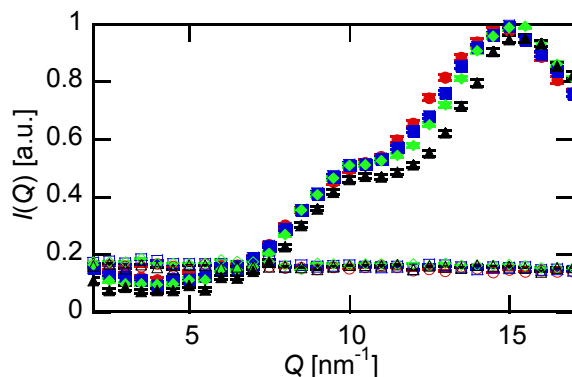


Figure 1. Neutron diffraction patterns of 3 mol/kg solution of LiPF_6/PC measured on the NSE spectrometer are plotted as a function of wavenumber, Q . The temperatures of the measurements were 320 K (red), 298 K (blue), 270 K (green), and 240 K (black). The coherent and incoherent parts are shown with filled and open symbols, respectively. The result at 298 K was the same as that shown in Ref. [1514](#).

Figure 1 shows the static structure factor of 3 mol/kg solution at various temperatures, which were determined using the NSE spectrometer. The results at other concentrations, including 0 mol/kg (neat solvent), are shown in Figs. S1a to S1c of Supporting Information. The variation of the structure factor is small particularly between 270 K and 320 K. A weak temperature dependence was observed also for the other concentrations.

The coherent structure factors exhibit a small shoulder at 10 nm^{-1} , which is hereafter called "prepeak", in addition to the main peak at 14 nm^{-1} . The height of the prepeak decreases with decreasing the concentration, as is shown in Figs. 1 and S1a to S1c. Very recently, some of us revealed with the neutron diffraction with isotope substitution and molecular dynamics simulation techniques that the prepeak originates in the domain structure composed of the ionic and the nonpolar parts,³² as in the case of ionic liquids with long alkyl chains.^{33,34,35,36,37} The intermediate scattering functions were measured at $Q = 10 \text{ nm}^{-1}$ and 14 nm^{-1} , which correspond to the prepeak and the main peak, respectively.

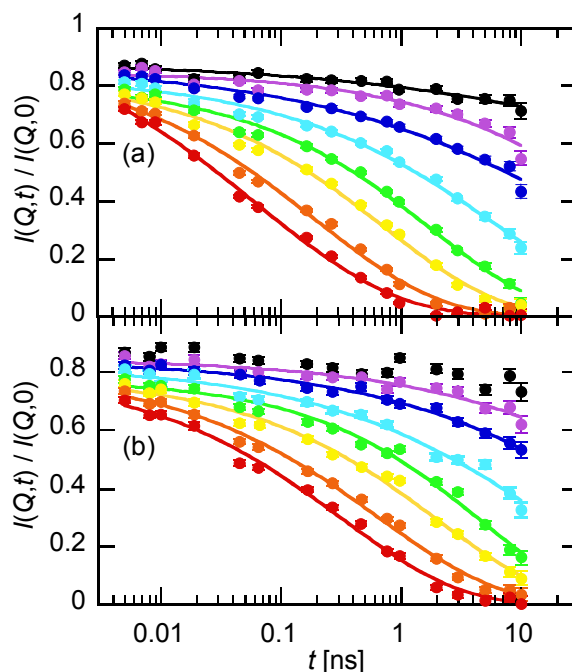


Figure 2. Intermediate scattering functions of 3 mol/kg solution of LiPF₆/PC at (a) $Q = 14 \text{ nm}^{-1}$ and (b) $Q = 10 \text{ nm}^{-1}$. The temperatures of the measurements were 320 K (red), 310 K (orange), 298 K (yellow), 290 K (green), 280 K (aqua), 270 K (blue), 260 K (purple), and 250 K (black). The experimental data are shown with filled circles with error bars, while the fitting lines of the KWW function, eq. 1, are shown with solid curves.

The normalized intermediate scattering functions at $Q = 14 \text{ nm}^{-1}$ (main peak) and $Q = 10 \text{ nm}^{-1}$ (prepeak) are shown in Figs. 2a and 2b, respectively, for 3 mol/kg solution, and those at other concentrations are in Figs. S2a to S4b of Supporting Information. The results at 298 K are the same as those in Ref. [1514](#). The relaxation of the intermediate scattering function becomes slower with decreasing temperature at all the concentrations as is expected. At the same temperature, the relaxation becomes slower with increasing the concentration of the salt, which is in harmony with the increase in steady-state shear viscosity. The relaxation at the prepeak is slower than that at the main peak except for the neat solvent, which exhibits no prepeak structure.

The intermediate scattering functions at two wavenumbers were approximated by the Kohlrausch-Williams-Watts (KWW) function as

$$\frac{I(Q,t)}{I(Q,0)} = A \exp\left[-\left(\frac{t}{\tau}\right)^\beta\right]. \quad (1)$$

All the three parameters, A , τ , and β , were treated as free adjustable parameters except for $I(Q,t)$ of the neat solvent at $Q = 10 \text{ nm}^{-1}$, where only the slowest tail of the intermediate scattering function was accessible by our NSE experiment as is shown in Fig. S4b. The value of A was fixed to be 0.85 for $I(Q,t)$ of neat PC at $Q = 10 \text{ nm}^{-1}$, which is a typical value at other conditions as will be shown later, and the other two parameters, β and τ , were optimized.

The parameters A and β , which represent the amplitude and the distribution of the relaxation times, respectively, are plotted in Figs. S5 and S6 of Supporting Information as the function of temperature. The amplitude A lies around 0.8 to 0.9 at all the temperatures and concentrations, except for higher temperature regions where the relaxation of the intermediate scattering function is fast and the initial part of the relaxation function was not observed within the time window of our NSE experiment. The error in A under such conditions is large, and β also suffers large errors there. We thus consider that the time window was not sufficient under these conditions to determine the three parameters simultaneously. The values of β scatters around 0.5, except for those of 1 mol/kg solution at $Q = 10 \text{ nm}^{-1}$. Since the height of the prepeak is low at 1 mol/kg, the scattering at $Q = 10 \text{ nm}^{-1}$ originates both from the prepeak and the low- Q edge of the main peak. We consider that the apparent large distribution of the relaxation time (small β) there is to be ascribed to the overlap of these two contributions.

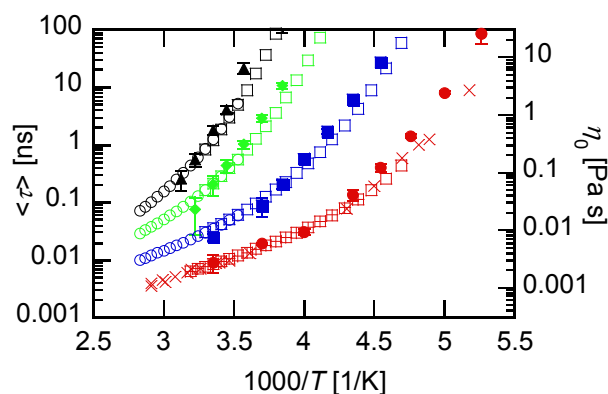


Figure 3. The mean relaxation time of the intermediate scattering function at $Q = 14 \text{ nm}^{-1}$, $\langle \tau \rangle$ (left axis), and the steady-state shear viscosity, η_0 (right axis), are plotted against the reciprocal temperature. The concentrations of the salt are 0 (red), 1 mol/kg (blue), 2 mol/kg (green), and 3 mol/kg (black), respectively. The mean relaxation times are plotted with filled symbols. The steady-state shear viscosity measured at CRIEPI and Nagoya University is shown with open circles and open squares, respectively. The steady-state shear viscosity values of neat PC reported in Refs. [2519](#) and [2620](#) are plotted with + and \times , respectively.

The mean relaxation time of the KWW function, $\langle \tau \rangle$, is defined as

$$\langle \tau \rangle \equiv \frac{\tau}{\beta} \Gamma\left(\frac{1}{\beta}\right), \quad (2)$$

where $\Gamma(x)$ stands for the gamma function. The mean relaxation times of the intermediate scattering functions were evaluated from the KWW fitting parameters through eq. 2. The values of $\langle \tau \rangle$ at $Q = 14 \text{ nm}^{-1}$ are plotted against the reciprocal temperature together with the steady-state shear viscosity, η_0 .

At ambient temperature, $1000/T = 3.3 \text{ K}^{-1}$, the increase in $\langle \tau \rangle$ with the salt concentration correlates with that in η_0 . We have demonstrated in our previous work that the shear relaxation spectra of LiPF₆/PC solutions at 2 mol/kg and 3 mol/kg are explained by the respective intermediate scattering functions at the main peak using MCT. The correlation between $\langle \tau \rangle$ and η_0 is thus quite natural, and it can be understood as that the structural relaxation at the main peak determines η_0 through the shear relaxation dynamics. Comparing the temperature dependences of $\langle \tau \rangle$ and η_0 , however, the slowing down of the former with decreasing the temperature is stronger than the increase in the latter at all the concentrations including the neat solvent.

There are two different ways to compare the temperature dependences of $\langle \tau \rangle$ and η_0 . The first one is to examine the proportionality between these two values as is performed in this work.¹⁰ This comparison stems from the Maxwell model of viscoelasticity as

$$\eta_0 = G_\infty \tau_\eta, \quad (3)$$

where G_∞ and τ_η stand for the high-frequency limiting shear modulus and the shear relaxation time.

Assumption of the temperature independence of the former yields the proportionality between η_0 and τ_η .

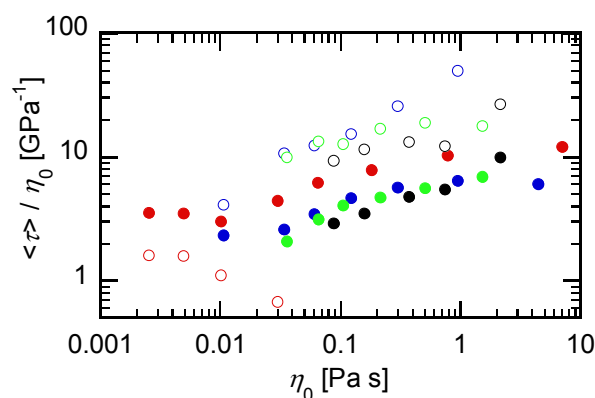
The second way of comparison is to expect the proportionality between τ and η_0 / T ,³⁸ which is deduced based on the following ideas. The relaxation time of the density mode, τ , is reciprocally proportional to a kind of diffusion coefficient, denoted as D , which is in turn related to η_0 by the Stokes-Einstein relationship as $D \propto T / \eta_0$. The combination of $\tau \propto 1/D$ and $D \propto T / \eta_0$ yields the proportionality between τ and η_0 / T .

In this work, we mainly employed the first idea and compared directly the temperature dependence of $\langle \tau \rangle$ and η_0 . We also tried the comparison between τ and η_0 / T , and the results are essentially the same as will be shown later.

The intermediate scattering functions are plotted against the time divided by the steady-state shear viscosity, t / η_0 , in Figs. S7a to S10b of Supporting Information in order to demonstrate the decoupling between η_0 and $\langle \tau \rangle$ in a different way. The formation of a master curve is not recognized, and the relaxation becomes slower with decreasing temperature on the t / η_0 axis except for neat PC at $Q = 10 \text{ nm}^{-1}$. It indicates that the temperature dependence of the relaxation time is stronger than that of the steady-state shear viscosity, and the decoupling between η_0 and $\langle \tau \rangle$ is not an artifact caused by the KWW analysis.

The relaxation time of the neutron intermediate scattering function of neat PC- h_6 was reported by Börjesson and Howells as a function of temperature.³⁹ The self-motion is mainly probed by the neutron quasi-elastic scattering of protonated samples due to the large incoherent scattering length of protons. Comparing their relaxation time at $Q = 16 \text{ nm}^{-1}$ with ours at $Q = 14 \text{ nm}^{-1}$, it should be noticed at first that the absolute value of the former is far smaller than the latter. The relaxation time of PC- d_6 is about 1 ns at 210 K ($1000/T = 4.8 \text{ K}^{-1}$), while that of PC- h_6 at the corresponding temperature is about 100 ps. In addition, the temperature dependence of the relaxation time of PC- h_6 is a little weaker than that of the

1 steady-state shear viscosity, which is opposite to our present results on neat PC- d_6 . The different
2 tendencies in PC- d_6 and PC- h_6 suggests the difference between the self- and the collective parts of the
3 intermediate scattering function, although the larger value of Q in PC- h_6 experiments may be a reason of
4 intermediate scattering function, although the larger value of Q in PC- h_6 experiments may be a reason of
5 faster relaxation and the intramolecular dynamics of the methyl group may contribute to the incoherent
6 intermediate scattering function of PC- h_6 . The self-part of the intermediate scattering function is often
7 used in computational studies for the evaluation of the structural relaxation time, mainly due to the
8 relative ease for the calculation of the self-part. However, since the coupling between the shear stress
9 and the collective density modes is considered in MCT, our present result underscores the importance of
10 the numerical evaluation of the collective part.



21
22
23
24
25
26
27
28
29
30
31
32
33
34
35
36 Figure 4. The mean relaxation times of the intermediate scattering function at the prepeak ($Q = 10 \text{ nm}^{-1}$,
37 open) and the main peak ($Q = 14 \text{ nm}^{-1}$, filled) divided by the steady-state shear viscosity are plotted as
38 the function of the steady-state shear viscosity. The concentrations of the salt are 0 (red), 1 mol/kg
39 (blue), 2 mol/kg (green), and 3 mol/kg (black), respectively.

46 The mean relaxation times at both wavenumbers are divided by η_0 and plotted against η_0 in Fig. 4.
47 The data points of $\langle \tau \rangle > 100 \text{ ns}$ were excluded from the plot because they involve large errors. The
48 ratios of $\langle \tau \rangle$ to η_0 are an increasing function of η_0 at both wavenumbers and all the concentrations
49 except for that of neat PC at $Q = 10 \text{ nm}^{-1}$. The magnitude of the increase depends little on the
50 wavenumber and the salt concentrations. In short, the structural relaxation of neat PC and LiPF₆/PC
51
52
53
54
55
56
57
58
59
60

solutions is decoupled from the steady-state shear viscosity, and the former exhibits stronger temperature dependence than the latter.

The longitudinal axis of Fig. 4 is changed to $\langle \tau \rangle T / \eta_0$ in Fig. S11 in order to test the proportionality between $\langle \tau \rangle$ and η_0 / T . The ratio is still an increasing function of η_0 , although the slope is a little smaller than that in Fig. 4. The decoupling between the structural relaxation time and the steady-state shear viscosity is thus evident in the comparison between $\langle \tau \rangle$ and η_0 / T , as well.

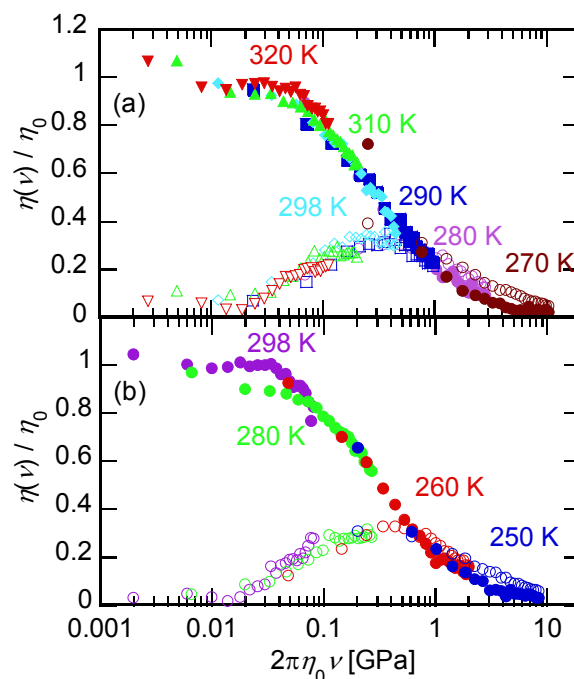


Figure 5. The normalized shear relaxation spectra, $\eta(\nu)/\eta_0$, are plotted against the frequency reduced to η_0 . The concentrations of the salt are (a) 3 mol/kg and (b) 2 mol/kg, respectively. The real and imaginary parts are shown with the filled and the open symbols, respectively. The spectra at different temperatures are shown with different colors, and the correspondence between the temperatures and the colors are indicated within the panels.

The steady-state shear viscosity is approximately given by the product of the shear relaxation time and the high-frequency limiting shear modulus as is described in eq. 3. The coupling between the structural relaxation and the shear viscosity usually means that the shear relaxation time is proportional to the structural relaxation time, with a constant limiting shear modulus. The assumption of the constant

1 limiting shear modulus does not necessary hold, however, and we need to examine the temperature
2 dependence of the shear relaxation time before discussing the decoupling between $\langle\tau\rangle$ and η_0 .
3
4

5 The shear relaxation time of viscous liquids can be probed through the measurement of the frequency-
6 dependent complex shear viscosity, that is, shear relaxation spectrum. We measured in this work the
7 shear relaxation spectra of the solutions of 2 mol/kg and 3 mol/kg at various temperatures in order to
8 examine the temperature dependence of the limiting shear modulus.
9
10
11
12
13

14 The normalized shear relaxation spectra are shown as the function of the reduced frequency in Figs. 5a
15 and 5b. The spectra at different temperatures reduce to a master curve at both concentrations when
16 plotted against the frequency reduced to η_0 , contrary to what seen with the intermediate scattering
17 functions shown in Figs. S7a and S8a of Supporting Information. In addition, the master curves at the
18 two concentrations resemble each other. From the peaks of the imaginary parts, the reduced relaxation
19 frequency is about 0.3 GPa. Since the peak frequency of the imaginary part approximately satisfies
20 $2\pi\nu\tau_{\eta}\sim 1$, the value of 0.3 GPa can be regarded as G_{∞} according to eq. 3. The reduction to the master
21 curve indicates that the shear relaxation time is proportional to the steady-state shear viscosity, implying
22 small variations of the limiting shear modulus. The decoupling between $\langle\tau\rangle$ and η_0 observed in Figs. 3
23 and 4 is thus regarded as that between the dynamics of the shear stress and the density modes at the
24 molecular scale.
25
26
27
28
29
30
31
32
33
34
35
36
37
38
39
40

41 The relationship between the relaxation times of the intermediate scattering function at the main peak
42 and the steady-state shear viscosity has been studied on some viscous liquids experimentally. The
43 proportionality between the structural relaxation time and the steady-state shear viscosity was confirmed
44 on representative supercooled liquids including glycerin and *o*-terphenyl.^{54,65,76} The shear relaxation
45 measurement by one of us recently demonstrated that the proportionality also holds between the
46 relaxation times of the density mode and the shear stress.⁴⁰ On the other hand, the larger temperature
47 dependence of the former than that of the latter, as is observed in our present work, was also reported on
48 LiCl/D₂O by Pravel and coworkers.¹¹⁴⁰ Some computational studies suggested a weaker temperature
49
50
51
52
53
54
55
56
57
58
59
60

1 dependence of the density mode relaxation,^{13+2,14+3} although such a decoupling has not been observed
2
3 experimentally to the best of our knowledge.
4

5 One may suspect that the stronger temperature dependence of the structural relaxation time may have
6 something to do with the presence of ions, because it is common to both LiPF₆/PC and LiCl/D₂O
7 solutions. However, we have observed the same decoupling on neat PC without salts, and the degree of
8 the decoupling is as large as that of the electrolyte solutions. In addition, the decoupling between the
9 structural relaxation and the steady-state shear viscosity was not observed on ionic liquids, where the
10 concentration of ions is quite high.⁸⁷
11
12
13
14
15
16
17
18

19 The relationship between the structural relaxation and the shear viscosity has been studied as one of
20 the universal properties of supercooled liquids that govern the slow dynamics near the glass-transition
21 temperature. However, our present result suggests that the relationship might be rather specific to
22 individual systems, and we consider that extensive studies would be necessary to understand the
23 characteristics of the stress-structure decoupling in terms of microscopic structures and interactions.
24
25
26
27
28
29
30
31
32
33
34

35 4. Summary 36 37 38 39

40 The structural relaxations of LiPF₆/PC solutions were measured as functions of temperature at various
41 concentrations using NSE spectroscopy. The temperature dependence of the structural relaxation time
42 was stronger than that of the steady-state shear viscosity. The shear relaxation spectra indicate that the
43 temperature dependence of the steady-state shear viscosity is explained by that of the shear relaxation
44 time. It was thus revealed that the dynamics of the shear stress is decoupled from that of the density
45 mode at the main peak of the static structure factor in the cases of LiPF₆/PC solutions and neat PC.
46
47
48
49
50
51
52
53
54
55
56
57
58
59
60

Acknowledgments

This work is partly supported by the Japan Society for the Promotion of Science (JSPS), KAKENHI Grant Nos. 24550019 and 16K05514. Michihiro Nagao acknowledges funding support of cooperative agreement 70NANB15H259 from the National Institute of Standards and Technology (NIST), U.S. Department of Commerce. Access to NGA-NSE was provided by the Center for High Resolution Neutron Scattering, a partnership between NIST and the National Science Foundation under Agreement No. DMR-1508249. Travel expenses of Tsuyoshi Yamaguchi and Koji Yoshida for the NSE experiment performed using NGA-NSE at NIST, USA were supported by General User Program for Neutron Scattering Experiments, Institute for Solid State Physics, The University of Tokyo (proposal no. 14601), at JRR-3, Japan Atomic Energy Agency, Tokai, Japan.

Supporting Information

The Supporting Information is available free of charge via the Internet at <http://pubs.acs.org/>.

The static diffraction patterns and the intermediate scattering functions of LiPF₆/PC solutions at 0 mol/kg (neat solvent), 1 mol/kg and 2 mol/kg, the temperature dependence of the KWW parameters A and β , the intermediate scattering functions plotted against the reduced time, and $\langle \tau \rangle T / \eta_0$ as the function of η_0 .

REFERENCES

- 1
2
3
4
5 (1) Hansen, J.-P.; McDonald, I. R. *Theory of Simple Liquids*, 2nd ed.; Academic Press: London, U.K.,
6
7 1986.
8
9
10 (2) Boon, J.-P.; Yip, S. *Molecular Hydrodynamics*; Dover Publications: New York, 1991.
11
12
13 (3) Balucani, U.; Zoppi, M. *Dynamics of the Liquid State*; Clarendon Press: Oxford, U.K., 1994.
14
15
16
17 (4) Harrison, G. *The Dynamic Properties of Supercooled Liquids*; Academic Press: London, U.K.,
18
19 1976.
20
21
22 (5) Petry, W.; Bartsch, E.; Fujara, F.; Kiebel, M.; Sillescu, H.; Farago, B. Z. Dynamic anomaly in the
23
24 glass transition region of orthoterphenyl. *Physik B - Condensed Matter* **1991**, *83*, 175–184.
25
26
27
28 (6) Bartsch, E.; Fujara, F.; Legrand, J. F.; Petry, W.; Sillescu, H.; Wuttke, J. Dynamics in viscous
29
30 orthoterphenyl: Results from coherent neutron scattering. *Phys. Rev. E* **1996**, *52*, 738–745.
31
32
33
34 (7) Wuttke, J.; Petry, W.; Pouget, S. Structural relaxation in viscous glycerol: Coherent neutron
35
36 scattering. *J. Chem. Phys.* **1996**, *105*, 5177–5182.
37
38
39 (8) Yamamuro, O.; Yamada, T.; Kofu, M.; Nakakoshi, M.; Nagao, M. Hierarchical Structure and
40
41 Dynamics of an Ionic Liquid 1-Octyl-3-methylimidazolium Chloride. *J. Chem. Phys.* **2011**, *135*,
42
43 054508.
44
45
46
47 (9) Faraone, A.; Hong, K.; Kneller, L. R.; Ohl, M.; Copley, J. R. D. Coherent Dynamics of Meta-
48
49 Toluidine Investigated by Quasielastic Neutron Scattering. *J. Chem. Phys.* **2012**, *136*, 104502.
50
51
52
53
54
55
56
57
58
59
60

1
2 (10) Sillrén, P.; Matic, A.; Karlsson, M.; Koza, M.; Maccarini, M.; Fouquet, P.; Götz, M.; Bauer, Th.;
3
4 Gulich, R.; Lunkenheimer, P. et al. Liquid 1-Propanol Studied by Neutron Scattering, Near-Infrared,
5
6 and Dielectric Spectroscopy. *J. Chem. Phys.* **2014**, *140*, 124501.
7
8

9
10 (11) Prevel, B.; Dupuy-Philon, J.; Jal, J. F.; Legrand, J. F.; Chieux, P. Structural Relaxation in
11
12 Supercooled Glass-Forming Solutions: a Neutron Spin-Echo Study of LiCl, 6D₂O. *J. Phys. Cond. Matt.*
13
14 **1994**, *6*, 1279–1290.
15
16

17
18 (12) Kanaya, T.; Inoue, R.; Saito, M.; Seto, M.; Yoda, Y. Relaxation Transition in Glass-Forming
19
20 Polybutadiene as Revealed by Nuclear Resonance X-Ray Scattering. *J. Chem. Phys.* **2014**, *140*, 144906.
21
22

23
24 (13) Zangi, R.; Kaufman, L. Frequency-dependent Stokes-Einstein relation in supercooled liquids. *J.*
25
26 *Phys. Rev. E* **2007**, *75*, 051501.
27
28

29 (14) Kim, K.; Saito, S. Role of the Lifetime of Dynamical Heterogeneity in the Frequency-Dependent
30
31 Stokes–Einstein Relation of Supercooled Liquids. *J. Phys. Soc. Jpn.* **2010**, *79*, 093601.
32
33

34
35 (15) Yamaguchi, T.; Yonezawa, T.; Yoshida, K.; Yamaguchi, T.; Nagao, M.; Faraone, A.; Seki, S.
36
37 Relationship between Structural Relaxation, Shear Viscosity, and Ionic Conduction of LiPF₆/Propylene
38
39 Carbonate Solutions. *J. Phys. Chem. B* **2015**, *119*, 15675–15682.
40
41
42

43 (16) Hayamizu, K.; Aihara, Y.; Arai, S.; Martinez, C. G. Pulse-Gradient Spin-Echo ¹H, ⁷Li, and ¹⁹F
44
45 NMR Diffusion and Ionic Conductivity Measurements of 14 Organic Electrolytes Containing
46
47 LiN(SO₂CF₃)₂. *J. Phys. Chem. B* **1999**, *103*, 519–524.
48
49
50

51 (17) Aihara, Y.; Sugimoto, K.; Price, W. S.; Hayamizu, K. Ionic Conduction and Self-Diffusion Near
52
53 Infinitesimal Concentration in Lithium Salt-Organic Solvent Electrolytes. *J. Chem. Phys.* **2000**, *113*,
54
55 1981–1991.
56
57
58
59
60

1
2 (18) Wuttke, J.; Ohl, M.; Goldammer, M.; Roth, S.; Schneider, U.; Lunkenheimer, P.; Kahn, R.;
3
4 Rufflé, B.; Lechner, R.; Berg, M. A. Propylene carbonate reexamined: Mode-coupling β scaling
5
6 without factorization? *Phys. Rev. E* **2000**, *61*, 2730–2740,
7
8

9
10 (19) Schneider, U.; Lunkenheimer, P.; Brand, R.; Loidl, A. Broadband dielectric spectroscopy on
11
12 glass-forming propylene carbonate. *Phys. Rev. E* **1999**, *59*, 6924–6936.
13
14

15
16 (20) Barthel, J.; Buchner, R.; Hölzl, C. G.; Münsterer, M. Dynamics of Benzonitrile, Propylene
17
18 Carbonate and Butylene Carbonate: the Influence of Molecular Shape and Flexibility on the Dielectric
19
20 Relaxation Behaviour of Dipolar Aprotic Liquids. *Z. Phys. Chem.* **2000**, *214*, 1213–1231.
21
22

23
24 (21) Brodin, A.; Frank, M.; Wiebel, S.; Shen, G.; Wuttke, J.; Cummins, H. Z. Brillouin-scattering
25
26 study of propylene carbonate: An evaluation of phenomenological and mode coupling analyses. *Phys.*
27
28 *Rev. E* **2002**, *65*, 051503.
29
30

31
32 (22) Qi, F.; Schun, K. U.; Dupont, S.; Döβ, A.; Böhmer, R.; Sillescu, H.; Kolshorn, H.; Zimmermann,
33
34 H. Structural relaxation of the fragile glass-former propylene carbonate studied by nuclear magnetic
35
36 resonance. *J. Chem. Phys.* **2000**, *112*, 9455–9462.
37
38

39
40 (23) Rosov, N.; Rathgeber, S.; Monkenbusch, M. Neutron Spin Echo spectroscopy at the NIST Center
41
42 for Neutron Research. *ACS Symp. Ser.* **2000**, *739*, 103–116.
43
44

45
46 (24) Azuah, R. T.; Knelle, L. R.; Qiu, Y.; Tregenna-Piggott, P.L.W.; Brown, C. M.; Copley, J. R. D.;
47
48 Dimeo, R. M. DAVE: A Comprehensive Software Suite for the Reduction, Visualization, and Analysis
49
50 of Low Energy Neutron Spectroscopic Data. *J. Res. Natl. Inst. Stand. Technol.* **2009**, *114*, 341–358.
51
52

53
54 (25) Barthel, J.; Gores, H.-J.; Carlier, P.; Feuerlein, F.; Utz, M. The Temperature Dependence of the
55
56 Properties of Electrolyte Solutions. V. Determination of the Glass Transition Temperature and
57
58
59
60

1
2 Comparison of the Temperature Coefficients of Electrolyte Conductance and Solvent Viscosity of
3
4 Propylene Carbonate Solutions. *Ber. Bunsenges. Phys. Chem.* **1983**, *87*, 436–443.

5
6
7
8 (26) Bondeau, A.; Huck, J. Etude de la viscosité de cisaillement des liquides sous-refroidis jusqu'à
9
10 leur température de transition vitreuse. Analyse des variations thermiques des coefficients de Vogel-
11
12 Fulcher. - I. Carbonate de propylène. (in French) *J. Phys.* **1985**, *46*, 1717–1730.

13
14
15
16 (27) Eisenberg, D.; Kauzmann, W. J. *The Structure and Properties of Water*; Clarendon Press:
17
18 London, U.K., 1969.

19
20
21 (28) Matsuo, S.; Makita, T. Isotope Effect on the Viscosity of Benzene and Cyclohexane Mixtures
22
23 Under High Pressures. *Int. J. Thermophys.* **1993**, *14*, 67–77.

24
25
26
27 (29) Behrends, R.; Kaatze, U. A High Frequency Shear Wave Impedance Spectrometer for Low
28
29 Viscosity Liquids. *Meas. Sci. Technol.* **2001**, *12*, 519–524.

30
31
32 (30) Yamaguchi, T.; Hayakawa, M.; Matsuoka, T.; Koda, S. Electric and Mechanical Relaxations of
33
34 LiClO₄-Propylene Carbonate Systems in 100 MHz Region. *J. Phys. Chem. B* **2009**, *113*, 11988–11998.

35
36
37
38 (31) Yamaguchi, T.; Mikawa, K.; Koda, S. Shear Relaxation of Water-Ionic Liquid Mixtures. *Bull.*
39
40 *Chem. Soc. Jpn.* **2012**, *85*, 701–705.

41
42
43 (32) Yamaguchi, T.; Yoshida, K.; Yamaguchi, T.; Kameda, Y.; Ikeda, K.; Otomo, T. Analysis of
44
45 Prepeak Structure of Concentrated Organic Lithium Electrolyte by Means of Neutron Diffraction with
46
47 Isotopic Substitution and Molecular Dynamics Simulation. *J. Phys. Chem. B* **2017**, *121*, 5355–5362.

48
49
50
51 (33) Lopes, J. N. A. C.; Pádua, A. A. H. Nanostructural Organization in Ionic Liquids. *J. Phys. Chem.*
52
53 *B* **2006**, *110*, 3330–3335.

1
2
3 (34) Russina, O.; Triolo, A. New Experimental Evidence Supporting the Mesoscopic Segregation
4 Model in Room Temperature Ionic Liquids. *Faraday Discuss.* **2012**, *154*, 97–109.

6
7
8 (35) Fujii, K.; Kanzaki, R.; Takamuku, T.; Kameda, Y.; Kohara, S.; Kanakubo, M.; Shibayama, M.;
9 Ishiguro, S.; Umebayashi, Y. Experimental Evidences for Molecular Origin of Low-Q Peak in
10 Neutron/X-Ray Scattering of 1-Alkyl-3-methylimidazolium Bis(trifluoromethanesulfonyl)amide Ionic
11 Liquids. *J. Chem. Phys.* **2011**, *135*, 244502.

13
14
15
16
17
18 (36) Shimizu, K.; Bernardes, C. E. S.; Lopes, J. N. C. Structure and Aggregation in the 1-Alkyl-3-
19 Methylimidazolium Bis(trifluoromethylsulfonyl)imide Ionic Liquid Homologous Series. *J. Phys. Chem.*
20 *B* **2014**, *118*, 567–576.

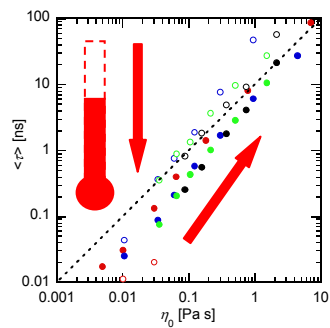
21
22
23
24
25
26 (37) Kashyap, H. K.; Hettige, J. J.; Annapureddy, H. V. R.; Margulis, C. J. SAXS Anti-Peaks Reveal
27 the Length-Scales of Dual Positive–Negative and Polar–Apolar Ordering in Room-Temperature Ionic
28 Liquids. *Chem. Commun.* **2012**, *48*, 5103–5105.

29
30
31
32
33
34 (38) Wuttke, J.; Petry, W.; Pouget, S. Structural relaxation in viscous glycerol: Coherent neutron
35 scattering. *J. Chem. Phys.* **1996**, *105*, 5177–5182.

36
37
38
39
40 (39) Börjesson, L.; Howells, W. S. Incoherent quasi-elastic neutron scattering of propylene carbonate
41 in the glass instability range. *J. Non-Cryst. Solids*, **1991**, *131–133*, 53–57.

42
43
44
45 (40) Yamaguchi, T. Experimental study on the relationship between the frequency-dependent shear
46 viscosity and the intermediate scattering function of representative viscous liquids. *J. Chem. Phys.*
47 **2016**, *145*, 194505.

TOC Graphic:

1
2
3
4
5
6
7
8
9
10
11
12
13
14
15
16
17
18
19
20
21
22
23
24
25
26
27
28
29
30
31
32
33
34
35
36
37
38
39
40
41
42
43
44
45
46
47
48
49
50
51
52
53
54
55
56
57
58
59
60